RESEARCH ARTICLE

The Inhibitory Neurotransmitter GABA Evokes Long-Lasting Ca^{2+} Oscillations in Cortical Astrocytes

Letizia Mariotti, Gabriele Losi, Michele Sessolo, Iacopo Marcon, and Giorgio Carmignoto

Studies over the last decade provided evidence that in a dynamic interaction with neurons glial cell astrocytes contribut to fundamental phenomena in the brain. Most of the knowledge on this derives, however, from studies monitoring the astrocyte Ca^{2+} response to glutamate. Whether astrocytes can similarly respond to other neurotransmitters, including the inhibitory neurotransmitter GABA, is relatively unexplored. By using confocal and two photon laser-scanning microscopy the astrocyte response to GABA in the mouse somatosensory and temporal cortex was studied. In slices from developing (P15-20) and adult (P30-60) mice, it was found that in a subpopulation of astrocytes GABA evoked somatic Ca^{2+} oscillations. This response was mediated by $GABA_B$ receptors and involved both $G_{i/o}$ protein and inositol 1,4,5-trisphosphate (IP_3) signalling pathways. *In vivo* experiments from young adult mice, revealed that also cortical astrocytes in the living brain exibit $GABA_B$ receptor-mediated Ca^{2+} elevations. At all astrocytic processes tested, local GABA or Baclofen brief applications induced long-lasting Ca^{2+} oscillations, suggesting that all astrocytes have the potential to respond to GABA. Finally, in patch-clamp recordings it was found that Ca^{2+} oscillations induced by Baclofen evoked astrocytic glutamate release and slow inward currents (SICs) in pyramidal cells from wild type but not $IP_3R2^{-/-}$ mice, in which astrocytic $GABA_B$ receptor-mediated Ca^{2+} elevations are impaired. These data suggest that cortical astrocytes in the mouse brain can sense the activity of GABAergic interneurons and through their specific recruitment contribut to the distinct role played on the cortical network by the different subsets of GABAergic interneurons.

GLIA 2016;64:363–373

Key words: GABAB receptor, calcium, somatosensory cortex, temporal cortex

Introduction

Over the last decade the glial cell astrocytes, beyond their broad control of brain tissue homeostasis and metabolism, have been recognized to regulate neuronal network activities (Araque et al., 2001; Carmignoto, 2000; Halassa et al., 2007; Haydon and Carmignoto, 2006; Perea et al., 2009; Volterra and Meldolesi, 2005). Indeed, astrocytes can modulate synaptic transmission and contribute to important phenomena in brain function thanks to a dynamic interaction with neurons that is finely regulated in time and space (Araque et al., 2014). It is now clear that astrocytes respond to the excitatory neurotransmitter glutamate with Ca^{2+} elevations mediated by metabotropic glutamate receptors (mGluR) and in response to this activation release various gliotransmitters, including glutamate, ATP, and D-serine that can exert multiple actions on neuronal communication, the nature of which depends on the specific type of targeted neuronal receptor and circuit. For example, astrocyte-derived glutamate can potentiate excitatory synaptic transmission through activation of presynaptic mGluR or N-methyl-D-aspartate (NMDA) receptors (Jourdain et al., 2007; Navarrete and Araque, 2010; Navarrete et al., 2012), but it can also favor neuronal synchronies by inducing slow inward currents mediated by postsynaptic NMDA receptors (D'Ascenzo et al., 2007;

View this article online at wileyonlinelibrary.com. DOI: 10.1002/glia.22933

Published online October 23, 2015 in Wiley Online Library (wileyonlinelibrary.com). Received July 20, 2015, Accepted for publication Sep 28, 2015.

Address correspondence to Giorgio Carmignoto; via U.Bassi 58/b, 35121 Padova, Italy. E-mail: gcarmi@bio.unipd.it

From the Neuroscience Institute, National Research Council (CNR) and Department of Biomedical Sciences, University of Padova, via U.Bassi 58/B, Padova, 35121, Italy

L. Mariotti and G. Losi contributed equally to this work.

Fellin et al., 2004; Pirttimaki et al., 2013). Whether astrocytes can similarly respond to other neurotransmitters such as GABA is relatively unexplored and of great importance (for reviews, see Losi et al., 2014; Velez-Fort et al., 2011). Indeed, although depending on a minority of all cortical neurons, GABAergic signaling plays fundamental roles in the brain as it governs the excitability of principal neurons and dynamically controls network activity across the brain, generating cortical oscillations and participating in signal integration and synaptic plasticity (Bartos et al., 2007; Cardin et al., 2009; Klausberger et al., 2003; Petersen and Crochet, 2013; Sohal et al., 2009; Stark et al., 2013; Varga et al., 2012). It is worth underline that studies in brain slices revealed that hippocampal astrocytes respond to exogenous GABA with Ca^{2+} elevations mediated by both $GABA_A$ and $GABA_B$ receptors (Meier et al., 2008), whereas astrocytes from the olfactory bulb exhibit Ca^{2+} elevations that appear to be mediated exclusively by GABA transporters (Kozlov et al., 2006). In the present study, we characterize the response of astrocytes to GABAergic signals in different cortical areas by using single and two-photon laser-scanning microscopy for Ca^{2+} imaging and patch-clamp recordings in both brain slice and *in vivo* preparations. A recruitment of astrocytes by GABAergic signals may have functional consequences different or complementary to the highly specialized roles that the different interneuron classes have in the regulation of the brain circuit activity.

Materials and Methods

Animals

All procedures were conducted in accordance with the Italian and European Communities Council Directive on Animal Care and were approved by the Italian Ministry of Health. We used C57BL/6J mice (both sexes) at postnatal days 15–20 (P15–20; young) and P35–60 (adults). We also used $IP_3R2^{-/-}$ mice (Li et al., 2005) and mice obtained by crossing GCaMP3 (B6;129S-*Gt(ROSA)26-Sortm38(CAG-GCaMP3)Hze*/J) and GLAST-CreERT2 mice (Mori et al., 2006). The expression of GCaMP3 was tamoxifen-inducible. Tamoxifen (SIGMA Aldrich, Milano, IT) was dissolved in corn oil (20 mg/mL stock solution) and injected intraperitoneally (1 mg/day) twice in young mice (P7–10) and for 5 days in adult (P30–35) mice. Mice were analyzed 10 days after the last tamoxifen-injection.

Brain Slice Preparation

Coronal slices of 350 μm containing somatosensory (SSCx) or temporal cortex (TeCx) were obtained from mice at postnatal days P15–20 and P30–60. Animals were anaesthetized with Zoletil (40 mg/kg, Virbac, Cedex, France) and Xilazyne (40 mg/kg, BIO98 srl, Barcelona, Spain) and the brain was removed and transferred into an ice-cold solution (ACSF, in mM: 125 NaCl, 2.5 KCl, 2 $CaCl_2$, 1 $MgCl_2$, 25 glucose, pH 7.4 with 95% O_2, and 5% CO_2). Coronal slices were cut with a vibratome (Leica Vibratome VT1000S Mannheim, Germany) in the solution described in Dugue et al. (2005). Slices were transferred for 1 minute in a solution at room temperature containing (in mM): 225 D-mannitol, 2.5 KCl, 1.25 NaH_2PO_4, 26 $NaHCO_3$, 25 glucose, 0.8 $CaCl_2$, 8 $MgCl_2$, 2 kynurenic acid with 95% O_2, and 5% CO_2. Slices were transferred in ACSF at 30°C for 20 minutes and then maintained at room temperature for the entire experiment.

Dye Loading

Brain slices were kept in ACSF with Sulforhodamine 101 (SR-101) (0.2 μM, Sigma Aldrich, Milano, Italy) at 30°C for 15 minutes to selectively stain astrocytes (Nimmerjahn et al., 2004) and then loaded for 15 minutes at 31°C with the Ca^{2+} sensitive dyes Fluo-4 AM (10 μM; Life Technologies, Monza, Italy). Loading mix containing sulfinpyrazone (200 μM, Sigma Aldrich, Milano, Italy), pluronic F-127 (0.12%, Sigma Aldrich, Milano, Italy), and kynurenic acid (1 mM, Sigma Aldrich, Milano, Italy) and was constantly bubbled with 95% O_2 and 5% CO_2.

Drug Applications

Drugs applied with bath perfusion were (in μM): GABA 200 (Tocris, Bristol, United Kingdom); Baclofen 20–50 (BAC; Tocris, Bristol, United Kingdom); SCH50911 20–50 (Tocris, Bristol, United Kingdom), CGP52432 2.5 (Abicam Biomedicals, United Kingdom), Muscimol 100 (MUS; Tocris, Bristol, United Kingdom), Picrotoxin 100 (PTX; SIGMA Aldrich, Milano, Italy), DHPG 20-50 (Tocris, Bristol, United Kingdom), D-AP5 50 (Abicam Biomedicals, United Kingdom), Tetrodotoxin 0.5–1 (TTX; Abcam, Cambridge, United Kingdom). A pressure ejection unit (PDES, NPI Electronics, Tamm, Germany) connected to a glass pipette (tip diameter 2–3 μm) containing GABA or BAC (both at 500 μM) was used for local drug applications (pressure 3 psi; duration 200 ÷ 600 ms). Pertussis toxin (PerTx; SIGMA Aldrich, Milano, Italy) was dissolved in ACSF (7.5 μg/mL) and slices were incubated for 3–5 hours.

Brain Slice Imaging Experiments

Slice imaging experiments were conducted with a confocal laser scanning microscope TCS-SP5-RS (Leica Microsystems, GmbH, Wetzlar, Germany) equipped with two lasers tuned at 488 nm and 550 nm or with a two photon laser scanning microscope Multiphoton Imaging System (Scientifica Ltd., Uckfield, East Sussex, United Kingdom) equipped with a pulsed infrared laser (Chameleon Ultra 2, Coherent, Santa Clara, CA) tuned at 780 or 910 nm. Power at sample was controlled in the range 5–10 mW. The excitation wavelengths used were: 488 or 780 nm for Fluo-4 AM and 488 or 910 nm for GCaMP3 for single or two photon excitation, respectively. Images were acquired at a resolution of 512 × 512 with at 1–2 Hz frame rate. Imaging was performed in cortical layers II–III and V and conducted at maximum for 1 hour with 1–2 minutes recording sessions every 5 minutes.

In Vivo Imaging Experiments

Mice were anaesthetized with an intraperitoneal injection of urethane ethylcarbamate (1.5 g/kg body weight, 10%; SIGMA Aldrich, Milano, Italy) solved in saline solution. Animal pinch withdrawal and eyelid reflex were tested to assay the depth of anesthesia. Dexamethasone sodium phosphate (2 mg/kg body weight, MSD,

Boxmeer, Netherlands) was injected intramuscularly to reduce cortical stress response during surgery and prevent cerebral oedema. Dextran TRITC (20 μL; Sigma Aldrich, Milan, Italy) was injected in caudal vein to selectively mark blood vessel. Body temperature was maintained at 37°C with a feedback-regulated heating pad. We monitored the respiration rate, heart rate and core body temperature throughout the experiment. The mouse was head-fixed and a craniotomy of 2–3 mm in diameter was drilled over the SSCx (AP 2.5 mm from bregma; ML 3.3 mm). The dura was carefully removed and the craniotomy was immediately covered with a coverslip with a hole. Warm HEPES-buffered artificial cerebrospinal fluid (ACSF, in mM: NaCl, 125; KCl, 5; glucose, 10; HEPES, 10; $MgSO_4$ 2; and $CaCl_2$, 2; at [pH 7.4]) filled the chamber to prevent desiccation and maintain ionic balance. To perform topical application of BAC, a borosilicate micropipette (Sutter instruments 1–2 μm tip diameter) was positioned over the hole on the coverslip. Imaging was performed with a two-photon microscope (Ultima IV, Prairie Technology now Bruker, USA) at 910 nm with a Chameleon 2 laser (see above). Imaging was performed at a resolution of 512 × 512 pixels in superficial layers (50–150 μm below the cortical surface) and acquired at 1–2 Hz. Imaging session lasted up to 2 hours with 1–2 minutes recording sessions every 5 minutes.

Electrophysiological Recordings

Brain slices were continuously perfused in a submerged chamber at a rate of 3–4 mL/min with (in mM): NaCl, 120; KCl, 2.5; NaH_2PO4, 1; $NaHCO_3$, 26; $MgCl_2$, 1; $CaCl_2$, 2; glucose, 10; at pH 7.4 (with 5% CO_2/95% O_2). Single and dual cell recordings were performed in voltage-clamp and current-clamp configuration using a multiclamp-700B amplifier (Molecular Devices, Foster City, CA) under the same microscopes as for slice imaging (see above). Signals were filtered at 1 kHz and sampled at 10 kHz with a Digidata 1440s interface and pClamp10 software (Molecular Devices, Foster City, CA). Typical pipette resistance was 3–4 MΩ. Access resistance was monitored throughout the recordings and was typically less than 25 MΩ. Whole-cell intracellular pipette solution was (in mM): K-gluconate, 145; $MgCl_2$, 5; EGTA, 0.5; Na_2ATP, 2; Na_2GTP, 0.2; HEPES, 10; to pH 7.2 with KOH, osmolarity, 280 ÷ 290 mOsm (calculated liquid junction potential: −14 mV). Pyramidal cells were identified on the basis of their distinct morphology and their response to hyperpolarizing and depolarizing 750 ms current steps. We selected only neurons showing a firing discharge with no spike amplitude accommodation (except for the second action potential in some cells), small after hyperpolarization and low steady-state frequency (15 ÷ 23 Hz with 200 pA current injection). SICs were recorded in Mg^{2+} free solution in presence of TTX, 1 μM (Abcam, Cambridge, UK) at a holding potential of −70 mV.

Data Analysis and Statistics

Data analysis was performed with Clampfit 10, Origin 8.0 (Microcal Software), Microsoft Office, ImageJ (NIH) and MATLAB 7.6.0 R2008A (Mathworks, Natick, MA). For imaging experiments, image sequences were aligned and processed with ImageJ and MATLAB. Region of interests (ROIs) were manually drawn around cellular body and processes using the red channel from the SR-101 signal. All pixels within each ROI were averaged to give a single time course $F(t)$. The Ca^{2+} signal for each ROIs was computed as $\Delta F/F_0 = (F(t) - F_0)/(F_0 - \text{background})$, where F_0 is the baseline fluorescence level obtained by averaging the fluorescence recorded during baseline activity. Peaks in the fluorescence were considered significant event when exceeding three standard deviation of the signal measured in baseline conditions. In electrophysiological experiments, inward currents with rise time (10%–90%) slower than 10 ms and amplitude greater than 20 pA were classified as SICs. The relative frequency of SICs was measured in the 5 minutes post pressure pulse applications (average of 1–3 applications, repeated every 5 minutes) then divided by each cell's control calculated in the period before BAC application (5 ÷ 25 minutes). For the analysis of other SICs parameters (rise, decay, duration, peak amplitude, and charge transferred) two minutes following BAC applications were considered.

According to data normal distribution we performed two-tailed Student's *t*-test for the percentage of active astrocytes and SIC frequency. Otherwise we used Wilcoxon test for Ca^{2+} peak frequency and Mann–Whitney test for SICs area, rise, decay, duration, and peak amplitude. Results were considered statistically significant when $^*P < 0.05$, $^{**}P < 0.01$, $^{***}P < 0.001$. All results are presented as mean ± s.e.m.

Results

Cortical Astrocytes Exhibit $GABA_B$ Receptor-Mediated Ca^{2+} Oscillations in Response to the Inhibitory Neurotransmitter GABA

We studied the response of astrocytes to GABA in slice preparations from the SSCx of young mice (P15–20) after incubation with the selective astrocytic marker SR-101 and the Ca^{2+} fluorescent indicator Fluo-4 AM (Fig. 1A,B). The Ca^{2+}-mediated fluorescence changes in astrocytes were recorded upon bath perfusion with GABA in the presence of TTX to block neuronal activity. At resting conditions a small fraction of astrocytes exhibited spontaneous Ca^{2+} transients at low frequency (Fig. 1D). Upon GABA applications, a significant number of cortical astrocytes showed a sustained Ca^{2+} response characterized by repetitive Ca^{2+} peaks (Fig. 1C1–3, D). To dissect out the GABA receptor involved in the astrocytic response, we next tested the effect of selective $GABA_A$ and $GABA_B$ receptor agonists and antagonists. We found that GABA-evoked Ca^{2+} responses in astrocytes were fundamentally unchanged in the presence of the selective $GABA_A$ receptor blocker PTX (Fig. 1C2, D), whereas both the frequency of Ca^{2+} oscillations and the number of active astrocytes were drastically reduced when GABA was applied in the presence of selective $GABA_B$ receptor antagonists (CGP 52432 and SCH 50911, Fig. 1C3, D). Consistent with a $GABA_B$ receptor-mediated response, the selective $GABA_A$ receptor agonist MUS failed to activate astrocytes (Fig. 1D). Conversely, the selective $GABA_B$ receptor agonist BAC induced Ca^{2+} elevations in astrocytes that were similar to those evoked by GABA (Fig. 1C4, D). Comparable results were also

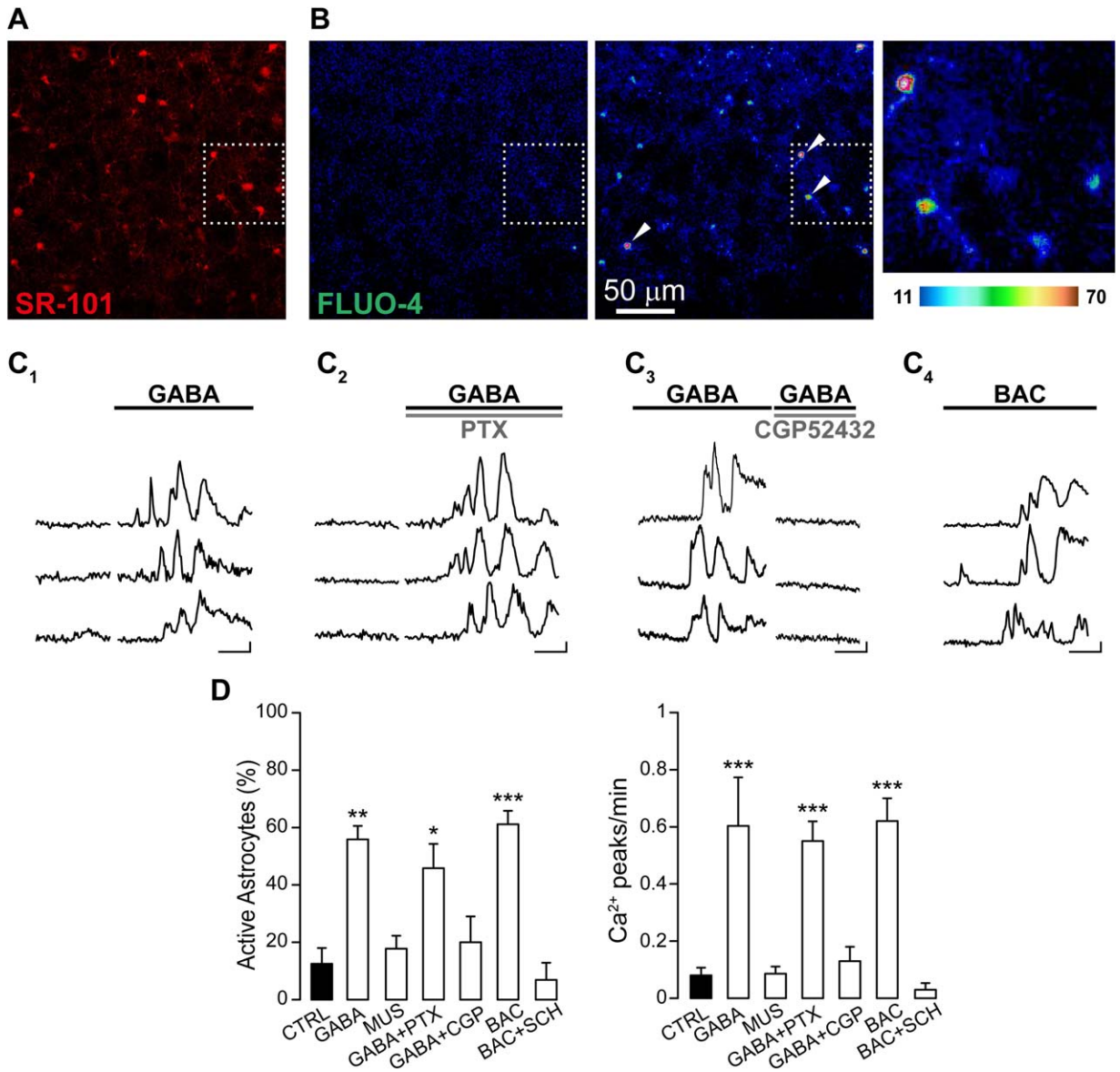

FIGURE 1: GABA activates somatic Ca^{2+} transients in astrocytes via $GABA_B$ receptor. (A) Red-fluorescent SR-101 selective labelling of astrocytes from SSCx. (B) Pseudo-colored images from FLUO-4 AM fluorescence signal acquired before (left) and after GABA applications in the presence of PTX (middle). The *white square* indicates the magnification with four astrocytic soma showing Ca^{2+} increases (right). Images are a maximal intensity projection of 35 frames. (C_{1-4}) Fluorescence signals over time from three astrocytes (indicated in B by *arrowheads*) in basal conditions and after perfusion with GABA (C_1), GABA and PTX (C_2), GABA and CGP 52432 (C_3) or BAC (C_4), respectively (scale bars: 50% $\Delta F/F_0$, 50 s). (D) Histograms showing the percentage of active astrocytes and the Ca^{2+} events frequency in different experimental conditions: GABA (76 astrocytes, 4 experiments; for percentage $P = 0.002$; for frequency $P = 1.97\ e^{-9}$), MUS (112 astrocytes, 5 experiments; for percentage $P = 0.644$; for frequency $P = 0.793$), GABA in presence of PTX (125 astrocytes, 5 experiments; for percentage $P = 0.015$; for frequency $P = 1.98\ e^{-9}$), GABA in presence of CGP 52432 (117 astrocytes, 9 experiments; for percentage $P = 0.451$, for frequency $P = 0.433$), BAC (99 astrocytes, 6 experiments; for percentage $P = 3.654\ e^{-5}$; for frequency $P = 2.24\ e^{-15}$), BAC in presence of SCH 50911 (112 astrocytes, 4 experiments; for percentage $P = 0.761$, for frequency $P = 0.500$).

obtained in slices from the TeCx where BAC evoked Ca^{2+} responses in 47.9% ± 12.1% of the astrocytes monitored (94 astrocytes, 4 experiments), suggesting that astrocyte responsiveness to GABA may be conserved in different neocortical regions. As in the SSCx, the astrocytic response in the TeCx was also prevented by the $GABA_B$ receptor antagonists SCH 50911 (data not shown).

$GABA_B$ receptor-Mediated Ca^{2+} Elevations in Astrocytes Depend on Activation of Both $G_{i/o}$ Protein and IP_3 Signaling

To clarify the cellular mechanism of $GABA_B$ receptor-mediated Ca^{2+} transients in astrocytes, we first tested the involvement of $G_{i/o}$ protein activation, because neuronal $GABA_B$ receptors are coupled to this subset of G-proteins

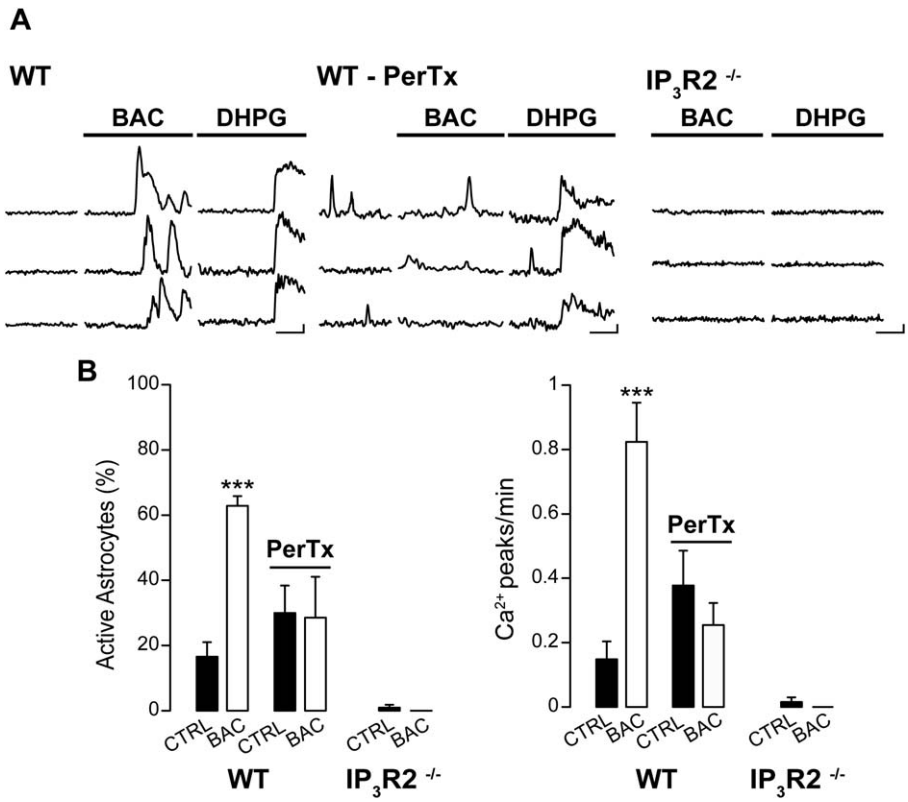

FIGURE 2: Astrocyte $GABA_BR$ activation recruits $G_{i/o}$ protein and IP_3 intracellular cascade. (**A**) Ca^{2+} signal changes from three representative astrocytes in response to BAC in control conditions (WT), after $G_{i/o}$ protein block by PerTx (WT-PerTx) and in transgenic mice lacking astrocytic inositol-1,4,5-trisphosphate ($IP_3R2^{-/-}$) signaling. As a control, we used DHPG that evoked Ca^{2+} increases in slices from WT, but not in $IP_3R2^{-/-}$ mice (scale bars: 50% $\Delta F/F_0$, 50 s). (**B**) Histograms showing the percentage of active astrocytes and the frequency of Ca^{2+} events per minute upon BAC applications, both in presence and in absence of PerTx (54 astrocytes in control conditions vs. 53 astrocytes treated with PerTx; 5 experiments; CTRL: for percentage $P = 0.00012$, for frequency $P = 1.19\ e^{-7,}$ PerTX: for percentage $P = 0.931$, for frequency $P = 0.185$) and in $IP_3R2^{-/-}$ mice (90 astrocytes, 7 experiments; for percentage $P = 0.337$, for frequency $P = 1$). In presence of PerTx, BAC failed to evoke astrocytic Ca^{2+} elevations.

(Bettler et al., 2004). Slices loaded with Fluo-4 AM and the selective astrocytic marker SR-101 were incubated with the $G_{i/o}$ blocker PerTx. We found that PerTx occluded in astrocytes the BAC-induced Ca^{2+} events, but not those evoked by DHPG, an agonist of the metabotropic glutamate receptor 1 and 5 associated with Gq-protein and IP_3 intracellular

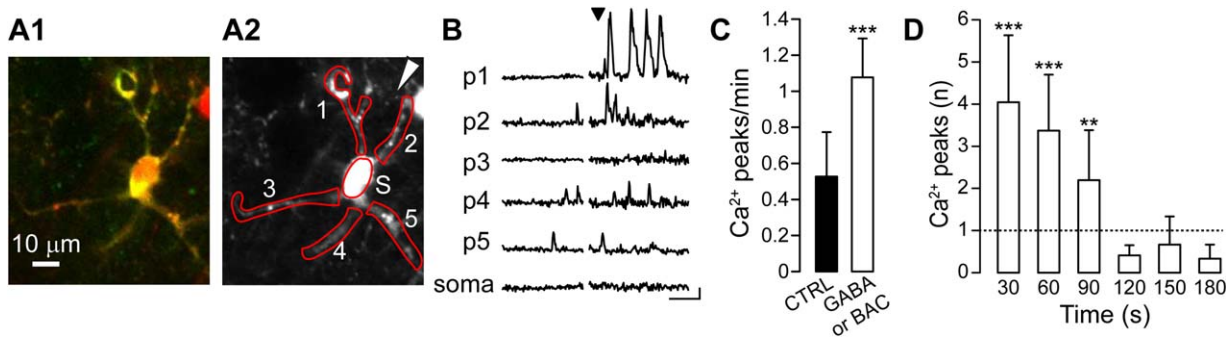

FIGURE 3: GABA activates long lasting Ca^{2+} transients in astrocytic processes. (A_1) Two-photon Ca^{2+} imaging of an astrocyte expressing the genetically encoded Ca^{2+} indicator $GCaMP_3$ and loaded with SR-101. Merged picture in which GCaMP3 and SR-101 positive astrocyte appear in yellow. (A_2) Mean intensity projection from SR-101 signal. Red ROIs highlight five primary processes and the soma, white arrowhead indicates the position of the pipette. (**B**) Ca^{2+} traces before and after local BAC applications (*black arrowhead*) from the five processes in A_2 (1–5) and from the soma (s; scale bars: 20% $\Delta F/F_0$, 50 s). (**C**) Histograms of Ca^{2+} peak frequency before and after GABA or BAC applications (pooled data, 89 primary processes from 16 astrocytes, 9 experiments; for frequency $P = 2.85\ e^{-6}$). (**D**) Mean number of Ca^{2+} peaks at different times after the brief GABA or BAC applications. The number was normalized to the mean value of Ca^{2+} oscillations observed in basal conditions and represented by the grey dotted line. Each period corresponds to a bin of 30 s (for 30 s, $P = 8.08\ e^{-6}$; for 60 s, $P = 3.82\ e^{-6}$; for 90, $P = 0.009$).

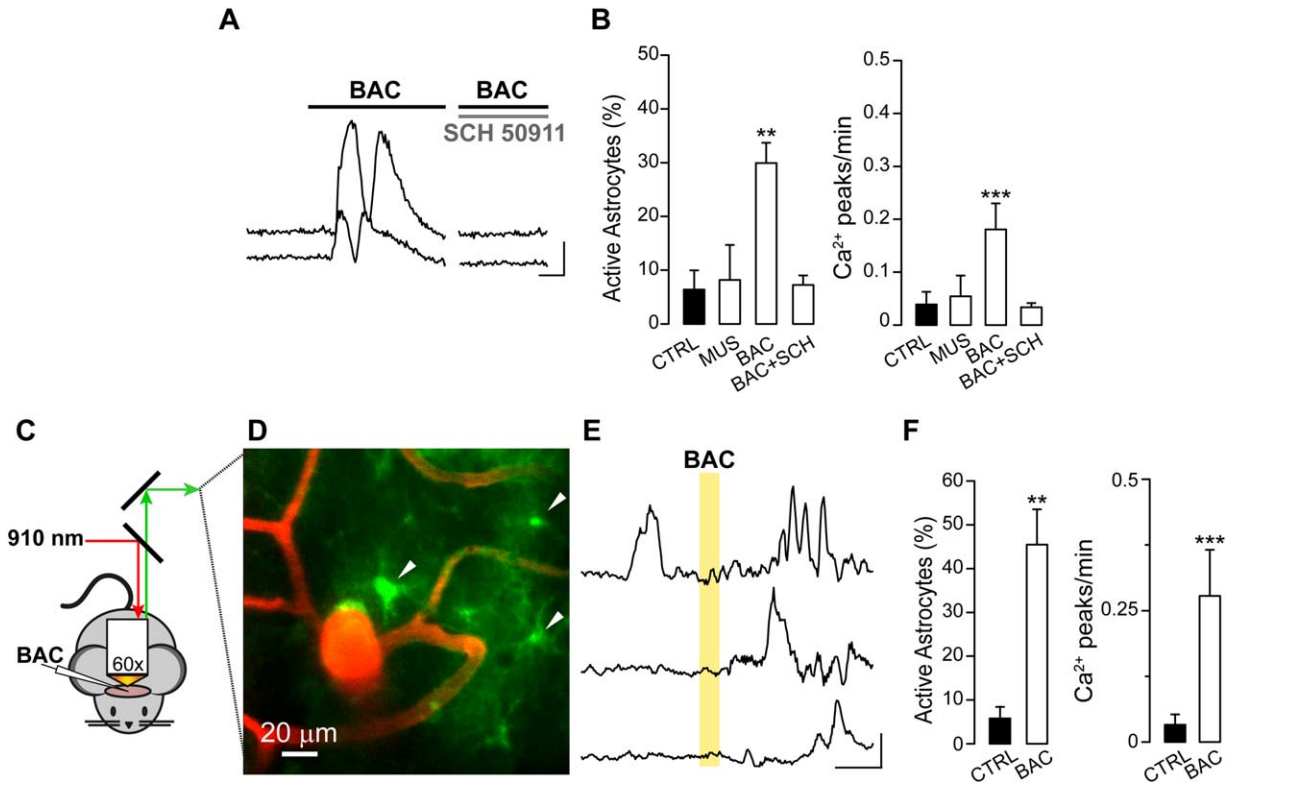

FIGURE 4: Local BAC applications trigger astrocyte Ca^{2+} transients in GCaMP3 adult mice. (A,B) Experiments in brain slices. (A) Fluorescence signals over time from two representative astrocytes acquired in basal conditions and after application of BAC alone or BAC with SCH 50911 (scale bars: 50% $\Delta F/F_0$, 50 s). (B) Histograms showing the percentage of active astrocytes and the Ca^{2+} event frequency in different experimental conditions: MUS (48 astrocytes, 4 experiments; for percentage $P = 0.915$, for frequency $P = 1$), BAC (92 astrocytes, 6 experiments; for percentage $P = 0.004$, for frequency $P = 1.51e^{-5}$), SCH 50911 (30 astrocytes, 2 experiments; for percentage $P = 0.151$, for frequency $P = 1$). (C–F) Experiments in anaesthetized mice. (C) Schematic representation of the two-photon *in vivo* set up. The excitation wavelength 910 nm excites both Dextran-TRITC and GCaMP3. (D) Maximal projection of blood vessels filled with Dextran-TRITC and astrocytes expressing GCaMP3 in layer I/II of SSCx (right). *White arrowheads* indicate three representative astrocytes soma. (E) Ca^{2+} traces before and after a BAC application. *Yellow area* marks the local BAC application (scale bars: 20% $\Delta F/F_0$, 50 s). (F) Summarizing histograms showing the percentage of active astrocytes and the Ca^{2+} events frequency in control conditions and after BAC applications (72 astrocytes, 4 animals; for percentage $P = 0.003$, for frequency $P = 9.61\ e^{-7}$).

signalling pathway (Fig. 2A, B), indicating that $G_{i/o}$-protein activation is necessary for BAC-induced Ca^{2+} elevations (Fig. 2A). We then evaluated whether the IP_3 pathway could also be involved by using SSCx and TeCx slices obtained from IP_3 receptor type 2-deficient mice ($IP_3R2^{-/-}$). The expression of this receptor in the brain is confined mainly, if not exclusively, to astrocytes in which it mediates the release of Ca^{2+} from endoplasmic reticulum (Hertle and Yeckel, 2007; Holtzclaw et al., 2002; Sharp et al., 1999). We first confirmed that the intracellular somatic Ca^{2+} elevations mediated by IP_3 signaling pathway are impaired in these mice, applying DHPG that failed to evoke any Ca^{2+} response (Fig. 2A). We next observed that astrocytes from these slice preparations also failed to respond to BAC (Fig. 2A, B) suggesting that beside $G_{i/o}$-protein, in astrocytes $GABA_B$-receptor mediated Ca^{2+} signal changes in response to GABA depend also on IP_3 intracellular cascade.

The Response of Astrocytic Processes to GABA is Composed of Sustained Ca^{2+} Oscillations

To further characterize the response to GABAergic signals at the level of astrocytic processes, we imaged Ca^{2+} signal dynamics in SSCx slices obtained from mice expressing the genetically encoded Ca^{2+} indicator GCaMP3 selectively in astrocytes (GCaMP3::GLAST-CreERT2 mice, see "Materials and Methods" sections). After loading slices with SR-101, we quantified the number of cells positive for both SR-101 and GCaMP3 (Fig. 3A1). We found that 74.8% ± 5.6% of 116 SR-101 labeled astrocytes (8 experiments) also expressed GCaMP3. Most importantly, all GCaMP3-expressing cells were marked by SR-101 confirming their astrocytic identity. We then used brief pressure pulses (200–500 ms duration, 2–3 PSI) to apply BAC or GABA from a glass micropipette located 10–20 µm from the processes of interest (Fig. 3A2). We found that a single, brief $GABA_B$ receptor agonist

application induced repetitive Ca^{2+} peaks in processes that outlasted the stimulus duration for at least 90 seconds (Fig. 3B–D). Notably, GABA was regularly effective in inducing Ca^{2+} elevations at the level of the processes whereas the response to GABA bath applications at the level of the soma was observed only in a subpopulation of astrocytes.

The $GABA_B$ Receptor Evoked Response in SSCx Astrocytes is Conserved in the Living Brain of Adult Mice

We next asked whether the astrocyte response to $GABA_B$ receptor activation that we observed in cortical slices from young mice is maintained in adulthood. We found that in slices obtained from adult GCaMP3::GLAST-CreERT2 mice ($30 < P < 60$), BAC triggered Ca^{2+} transients similar to those observed in astrocytes from young mice, although the number of responsive astrocytes was lower with respect to that in slices from young animals (Fig. 4A, B; compare with Fig. 1). Also in adult slices, MUS failed to activate astrocytes (Fig. 4B) while the $GABA_B$ receptor antagonist SCH 50911 largely suppressed the astrocytic Ca^{2+} response to BAC (Fig. 4A, B).

To validate the results obtained in brain slice preparations, we performed two-photon Ca^{2+} imaging in the living brain of P30–60 anaesthetized GCaMP3 mice (Fig. 4C, D). We found that a large number of astrocytes from layer I/II of the primary SSCx responded to BAC applied to cortical surface with repetitive Ca^{2+} elevations (Fig. 4E, F).

GABA-Activated Astrocytes Release Glutamate That Evokes Pyramidal Neuron Firing Activity

We next investigated whether and how GABA-activated astrocytes signal back to neurons. In SSCx slices from young mice (P15–20), we performed single and dual cell patch-clamp recordings from pyramidal neurons in SSCx slices in the presence of TTX (1 μM) and nominally Mg^{2+} free solution to favor NMDA receptors activation. Under these conditions, we recorded low frequency glutamatergic SICs that we know to be due to spontaneous release of glutamate from astrocytes (Fellin et al., 2004). To avoid a sustained activation of neuronal $GABA_B$ receptors by bath applied BAC, we used local BAC pressure pulse applications (400–600 ms, 5–7 PSI). This stimulation evoked a hyperpolarizing current mediated by neuronal postsynaptic $GABA_B$ receptors in neurons located less than 100 μm from the BAC pipette tip (Fig. 5A, range 80 ÷ 150 μm; mean duration, 54 ± 9 s; $n = 10$ neurons). BAC applications also induced long-lasting Ca^{2+} oscillations in astrocytes (Fig. 3) and SICs in neurons with a frequency that remained increased with respect to control for 2 minutes after BAC applications (Fig. 5A, B). Spontaneous and BAC-induced SICs, in the 2 minutes following the application, had similar slow kinetics (rise 10%–90%: 94 ± 13 ms, $n = 60$, before and 90 ± 13 ms, $n = 38$, after BAC, $P = 0.897$; decay 90%–10%: 339 ± 46 ms, $n = 56$, before and 358 ± 54 ms, $n = 33$, after BAC, $P = 0.340$; duration: 0.78 ± 0.10 s, $n = 60$, before and 0.70 ± 0.10s; $n = 40$, after BAC, $P = 0.935$; 18 experiments), area (Fig. 5C) and peak amplitude (-75 ± 7 pA, $n = 59$ before and -101 ± 14 pA, $n = 40$, $P = 0.145$,; see also Fig. 5F). Similarly to what observed with other stimuli also BAC-induced SICs were mediated by NMDA receptors being strongly reduced by D-AP5 (50 μM; Fig. 5A, E; peak -28 ± 12 pA, $P = 0.0001$; $n = 9$, 5 experiments).

To assess whether BAC-evoked SICs depend on astrocytic Ca^{2+} elevations, we performed patch-clamp experiments in slices from $IP_3R2^{-/-}$ mice in which G-protein coupled Ca^{2+} elevations are impaired in astrocytes, as reported above (Fig. 2A). We found that in slices from $IP_3R2^{-/-}$ mice, BAC failed to increase SIC frequency in pyramidal neurons (Fig. 5C, E; 13 experiments). These data indicate that the increased SIC frequency observed in neurons upon BAC challenge is mediated by IP_3-mediated Ca^{2+} elevations in astrocytes.

In diverse brain regions including cortex, hippocampus and nucleus accumbens (D'Ascenzo et al., 2007; Fellin et al., 2004), pair recording experiments revealed that SICs can occur with a high degree of synchrony in contiguous pyramidal neurons. We thus tested whether BAC-evoked SICs could also occur synchronously in neighboring pyramidal neurons. To this aim, we performed patch-clamp recordings from pairs of adjacent pyramidal neurons (Fig. 5B; <100 μm apart) and found that after BAC application 8 out of 20 SICs recorded were synchronous (range 4 ÷ 74 ms from 2 paired recordings). Next, to assess the possibility that SICs could induce action potential firing in pyramidal cells, we first divided the amplitude of all SICs recorded to each cell's rheobase current. We found that SICs above rheobase were 58% in control and 67% following BAC applications (Fig. 5F). Finally, in dynamic clamp experiments we injected SICs in pyramidal neurons of increasing amplitude and duration in the absence of TTX. We found that 100 pA SIC evoked 1 to 2 action potentials in 3 out of 9 cells tested, while larger events evoked intense firing activity in all cells tested (Fig. 5G; 3.4 ± 0.4 and 11.4 ± 1.1 action potentials with SICs of 131 pA, $n = 9$, and 285 pA, $n = 8$, respectively).

Discussion

In the present study we provide evidence that a similar subpopulation of astrocytes from two cortical regions of the mouse brain, that is, the SSCx and the TeCx, responds to GABA with intracellular Ca^{2+} increases which depend on activation of both $GABA_B$ receptors and IP_3 intracellular signaling. These Ca^{2+} elevations have a marked tendency to oscillate for prolonged periods even after brief $GABA_B$ receptor activations and induce in astrocytes the release of the gliotransmitter

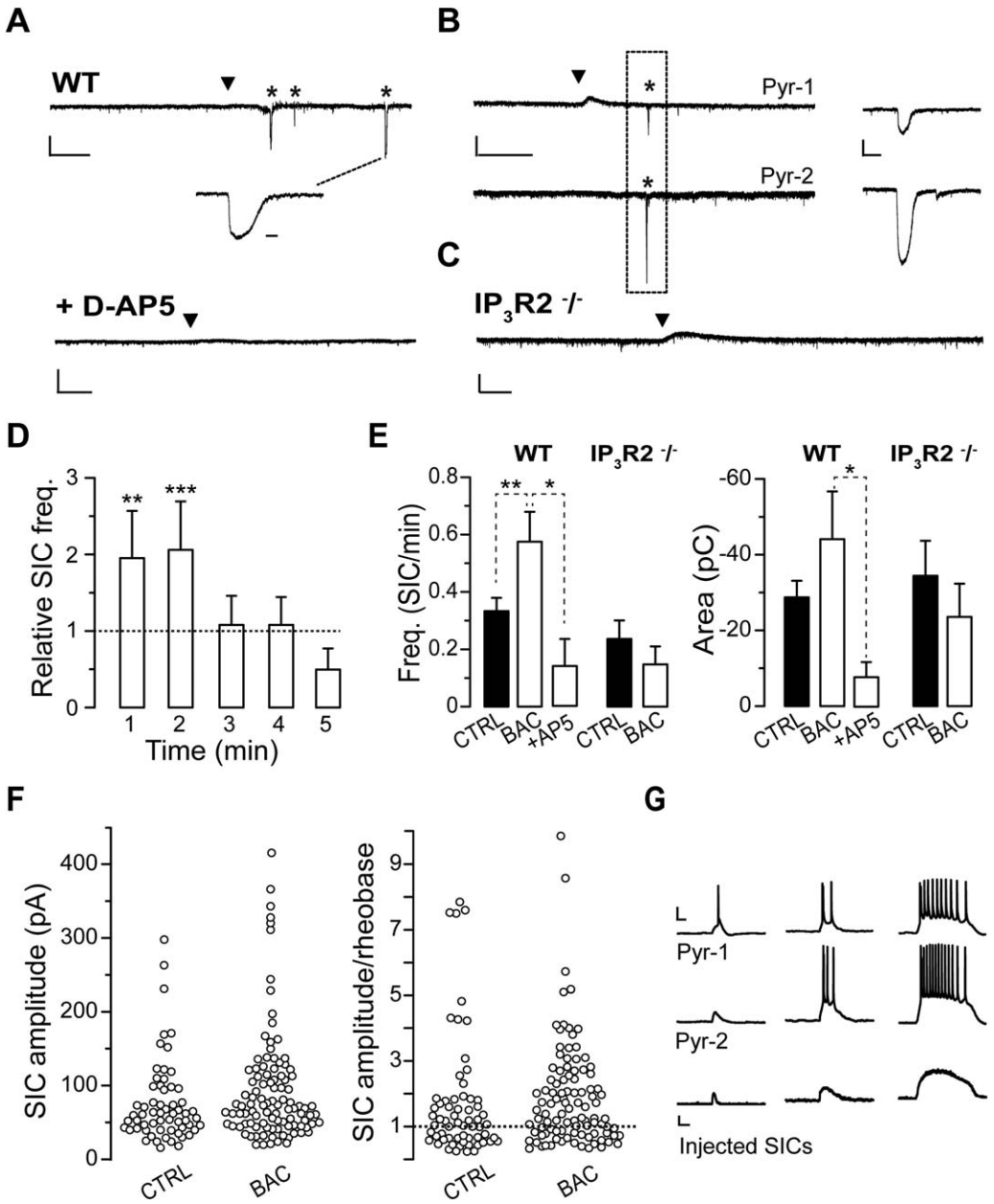

FIGURE 5: GABA-activated astrocytes evoke SICs in pyramidal neurons. (A–C) Representative whole cell currents from single pyramidal neurons (A) or a pair (C) of adjacent pyramidal neurons (90 μm apart; Pyr-1 and −2) showing the occurrence of SICs (*asterisks*) after a BAC local application (*black arrowheads*) to layer V SSCx in a WT mouse and the absence of SICs upon a similar BAC application in presence of D-AP5 (A) and in $IP_3R2^{-/-}$ mice (C). (Scale bars: For single recordings: 1 minute, 100 pA; enlarged SIC: 500 ms; for paired recording and D-AP5: 20 s, 100 pA and 2 s for the enlarged SIC. **(D)** The relative SIC frequency is significantly increased for 2 minutes following BAC application (see Methods; $n = 21$ cells, $P = 0.006$ and 0.001, for first and second minute, respectively). **(E)** Summary of SIC mean frequency and area before and after (2 minutes) local BAC applications in WT and $IP_3R2^{-/-}$ mice. (Frequency: for WT, $n = 21$ cells, $P = 0.010$; in presence of D-AP5, $P = 0.028$, $n = 5$ cells; for $IP_3R2^{-/-}$ mice, $n = 13$ cells; $P = 0.367$; Area: for WT mice, $n = 60$ SICs for control and 38 after BAC; $P = 0.407$; in presence of D-AP5, $P = 0.050$, $n = 9$ SICs; for $IP_3R2^{-/-}$ mice, $n = 30$ and 9 SICs for control and after BAC, respectively, $P = 0.536$). **(F)** Distribution of all SIC peak amplitude recorded before and after BAC applications (**left**) and ratio of each SIC peak amplitude to the action potential threshold (rheobase) in each cell (**right**). **(G)** Examples of membrane potential recordings (upper and middle traces) from two different pyramidal neurons (Pyr-1 and −2) during the injection of SICs of increasing size (lower traces, peak amplitudes of 100, 131, and 285 pA) show the occurrence of action potentials during SICs.

glutamate which evokes synchronous NMDAR-mediated depolarizing events in pyramidal neurons. Such a functional response of astrocytes to the inhibitory neurotransmitter GABA suggests that the recruitment of astrocytes may accompany the activity of the different classes of interneurons in the brain and have functional consequences on local network excitability.

Previous studies in cultured astrocytes (Nilsson et al., 1993) and hippocampal slices from young rats (Meier et al., 2008) described GABA-induced Ca^{2+} elevations in astrocytes that were mediated by both $GABA_A$ and $GABA_B$ receptors, while others reported in hippocampal astrocytes Ca^{2+} responses exclusively mediated by $GABA_B$ receptors (Kang et al., 1998; Serrano et al., 2006). Activation of $GABA_A$ receptors in astrocytes may lead to a membrane depolarization and increase the intracellular Ca^{2+} in these cells through voltage-operated calcium channel (VOCC) activation. In our experiments, however, we never observed astrocytic Ca^{2+} elevations upon a selective activation of the $GABA_A$ receptor. This discrepancy may possibly be ascribed to the different area, that is, cortex versus hippocampus, or species used, that is, mouse versus rats. Notably, however, while in cultures astrocytes can express VOCCs (Parpura et al., 2011; Verkhratsky et al., 2012; Verkhratsky and Steinhauser, 2000) and cells undergoing reactive astrogliosis in status epilepticus can exhibit measurable L- and P/Q channel activity (Westenbroek et al., 1998), whether astrocytes *in situ* express VOCCs remains unclear (Carmignoto et al., 1998). An additional mechanism that can indirectly favor astrocytic Ca^{2+} elevations in response to GABA has been revealed in slices from the developing olfactory bulb. There, an intense activity of the GABA transporters (GATs) is observed to cause a Na^+ overloading in the astrocytes which then leads to Ca^{2+} elevations due to an inverse operation of the Na^+/Ca^{2+} exchanger (Doengi et al., 2009). The fact that in our experiments GABA-mediated responses in astrocytes were abolished by $GABA_B$ receptor selective antagonists argues against a possible involvement of GATs in cortical astrocyte response to GABA.

In rat hippocampal astrocytes, a developmental profile of $GABA_B$ receptor-mediated astrocytic responses, with a peak between P11 and P15 and a marked decline after P21, has been described (Meier et al., 2008). In slices from young adult mice we found that the percentage of GABA-responsive astrocytes was only slightly reduced with respect to that observed in slices from P15–20 mice. In addition and most importantly, in specific *in vivo* experiments in anaesthetized adult GCaMP3 mice, we observed prompt Ca^{2+} elevations in layer I/II astrocytes of the SSCx in response to the $GABA_B$ receptor agonist BAC. All in all, our results provide evidence that from the early development to adulthood, neocortical astrocytes maintain their potential to respond to GABA with Ca^{2+} elevations and that their response is fundamentally mediated by $GABA_B$ receptor activation.

An additional observation that we describe here regards the mechanism at the basis of the astrocyte Ca^{2+} response to GABA. We reveal that the astrocytic response is sensitive to the $G_{i/o}$ blocker PerTx. We also reveal that in slices obtained from $IP_3R2^{-/-}$ mice $GABA_B$-mediated Ca^{2+} responses are also abolished which suggests an involvement of both signaling, that is, the $G_{i/o}$ protein and the IP_3-mediated intracellular pathway, in astrocytic GABA-induced Ca^{2+} elevations. The full intracellular cascade at the basis of the $GABA_B$ receptor-mediated intracellular Ca^{2+} increases remains, however, unclear. In general, astrocytic Ca^{2+} oscillations result from the activation of the G_q-coupled metabotropic receptor and IP_3 intracellular signaling cascade. It is possible that also $G_{i/o}$ protein signalling converges on the IP_3-signaling pathway. Indeed, it has been shown that activation of $G_{\beta/\gamma}$ complex can lead to stimulation of PLC_β1-3 (Pierce et al., 2002) or directly of IP_3 formation (Zeng et al., 2003). Alternatively, a specific interaction between $G_{i/o}$ and G_q protein could occur and mediate IP_3R2-dependent astrocytic responses. Notwithstanding these possible hypotheses, additional studies are necessary to fully elucidate the intracellular mechanism of the GABA-mediated Ca^{2+} response in astrocytes.

Elevations in the intracellular Ca^{2+} in response to GABA were observed not only at the level of the soma, but also at astrocytic processes that are, in principle, closer than the soma to GABAergic axon terminals. Consistent with the expression of $GABA_B$ receptors at these sites, in slices from GCaMP3::GLAST-CreERT2 mice we observed Ca^{2+} oscillations at these astrocytic processes upon a single, brief stimulation with GABA or BAC applied locally through a glass pipette. This response at the processes was observed even in absence of Ca^{2+} increases at the soma, and although they were induced by a brief stimulation, they were sustained for about two minutes, largely outlasting stimulus duration. These results suggest that, similarly to glutamate-mediated Ca^{2+} elevations, GABA-mediated Ca^{2+} elevations at the processes can be integrated by the astrocytes into a more global response that eventually includes the soma.

We found that GABA-activated astrocytes release glutamate which triggers in pyramidal cells NMDA receptor-mediated SICs. We also found that these events in the virtual absence of extracellular Mg^{2+} induce an intense action potential firing in these cells. In the presence of physiological extracellular Mg^{2+} SIC amplitude is, however, reduced (Fellin et al., 2004). Therefore, under physiological conditions only large amplitude SICs may induce a membrane depolarization in pyramidal cells sufficient to reach action potential threshold. Consistent with the sustained Ca^{2+} oscillations induced in astrocytes by GABA, SICs occurred for a few minutes, outlasting the time of GABA agonist applications. Notably, our data revealed that in slices from $IP_3R2^{-/-}$ mice $GABA_B$ receptor stimulation failed to evoke both Ca^{2+} elevations in astrocytes and SICs in pyramidal neurons, further validating the astrocytic origin and the Ca^{2+} dependency of GABA-evoked SICs. In line with previous observations from different brain regions (Angulo et al., 2004; Bardoni et al., 2010;

Cavelier and Attwell, 2005; D'Ascenzo et al., 2007; Fellin et al., 2004; Gomez-Gonzalo et al., 2010; Nestor et al., 2007; Pirttimaki et al., 2013; Reyes-Haro et al., 2010; Shigetomi et al., 2008), SICs were demonstrated to be mediated by NMDA receptors and to occur synchronously in adjacent pyramidal neurons. These observations suggest that astrocytes in response to a brief stimulation with the inhibitory neurotransmitter GABA, signal back to local circuits and by enhancing synchronized activity in pyramidal neurons turn a local transient inhibition into a delayed excitation.

In conclusion, in the present study we show that astrocytes from two different neocortical regions committed to different brain functions, that is, the SSCx and the TeCx of the mouse, have the potential to sense synaptic GABA and to respond to this signal with oscillatory Ca^{2+} transients and glutamate release that can affect local network activities. Our observations urge for additional studies that could specifically explore whether and how astrocytes are recruited by the different classes of GABAergic interneurons.

Acknowledgment

Grant sponsor: Telethon Italy; Grant number: GGP12265; Grant sponsor: Fondazione Cariparo; Grant sponsor: National Research Council Aging Project; Grant sponsor: Fondo Per gli Investimenti della Ricerca di Base; Grant number: RBAP11X42L.

We thank Alfonso Araque and Tommaso Fellin for the generous gift of $IP_3R2^{-/-}$ and GLAST-CreERT2 mice, respectively. We also thank Angela Chiavegato for help with *in vivo* procedures; Alessandra Tessari and Micaela Zonta for excellent technical support.

References

Angulo MC, Kozlov AS, Charpak S, Audinat E. 2004. Glutamate released from glial cells synchronizes neuronal activity in the hippocampus. J Neurosci 24:6920–6927.

Araque A, Carmignoto G, Haydon PG. 2001. Dynamic signaling between astrocytes and neurons. Annu Rev Physiol 63:795–813.

Araque A, Carmignoto G, Haydon PG, Oliet SH, Robitaille R, Volterra A. 2014. Gliotransmitters travel in time and space. Neuron 81:728–739.

Bardoni R, Ghirri A, Zonta M, Betelli C, Vitale G, Ruggieri V, Sandrini M, Carmignoto G. 2010. Glutamate-mediated astrocyte-to-neuron signalling in the rat dorsal horn. J Physiol 588(Pt 5):831−846.

Bartos M, Vida I, Jonas P. 2007. Synaptic mechanisms of synchronized gamma oscillations in inhibitory interneuron networks. Nat Rev Neurosci 8:45–56.

Bettler B, Kaupmann K, Mosbacher J, Gassmann M. 2004. Molecular structure and physiological functions of $GABA_B$ receptors. Physiol Rev 84: 835–867.

Cardin JA, Carlen M, Meletis K, Knoblich U, Zhang F, Deisseroth K, Tsai LH, Moore CI. 2009. Driving fast-spiking cells induces gamma rhythm and controls sensory responses. Nature 459:663–667.

Carmignoto G. 2000. Reciprocal communication systems between astrocytes and neurones. Prog Neurobiol 62:561–581.

Carmignoto G, Pasti L, Pozzan T. 1998. On the role of voltage-dependent calcium channels in calcium signaling of astrocytes in situ. J Neurosci 18: 4637–4645.

Cavelier P, Attwell D. 2005. Tonic release of glutamate by a DIDS-sensitive mechanism in rat hippocampal slices. J Physiol 564(Pt 2):397–410.

D'Ascenzo M, Fellin T, Terunuma M, Revilla-Sanchez R, Meaney DF, Auberson YP, Moss SJ, Haydon PG. 2007. mGluR5 stimulates gliotransmission in the nucleus accumbens. Proc Natl Acad Sci USA 104:1995–2000.

Doengi M, Hirnet D, Coulon P, Pape HC, Deitmer JW, Lohr C. 2009. GABA uptake-dependent Ca^{2+} signaling in developing olfactory bulb astrocytes. Proc Natl Acad Sci USA 106:17570–17575.

Dugue GP, Dumoulin A, Triller A, Dieudonne S. 2005. Target-dependent use of co-released inhibitory transmitters at central synapses. J Neurosci 25: 6490–6498.

Fellin T, Pascual O, Gobbo S, Pozzan T, Haydon PG, Carmignoto G. 2004. Neuronal synchrony mediated by astrocytic glutamate through activation of extrasynaptic NMDA receptors. Neuron 43:729–743.

Gomez-Gonzalo M, Losi G, Chiavegato A, Zonta M, Cammarota M, Brondi M, Vetri F, Uva L, Pozzan T de Curtis M, Ratto GM, Carmignoto G. 2010. An excitatory loop with astrocytes contributes to drive neurons to seizure threshold. PLoS Biol 8:e1000352.

Halassa MM, Fellin T, Haydon PG. 2007. The tripartite synapse: Roles for gliotransmission in health and disease. Trends Mol Med 13:54–63.

Haydon PG, Carmignoto G. 2006. Astrocyte control of synaptic transmission and neurovascular coupling. Physiol Rev 86:1009–1031.

Hertle DN, Yeckel MF. 2007. Distribution of inositol-1,4,5-trisphosphate receptor isotypes and ryanodine receptor isotypes during maturation of the rat hippocampus. Neuroscience 150:625–638.

Holtzclaw LA, Pandhit S, Bare DJ, Mignery GA, Russell JT. 2002. Astrocytes in adult rat brain express type 2 inositol 1,4,5-trisphosphate receptors. Glia 39:69–84.

Jourdain P, Bergersen LH, Bhaukaurally K, Bezzi P, Santello M, Domercq M, Matute C, Tonello F, Gundersen V, Volterra A. 2007. Glutamate exocytosis from astrocytes controls synaptic strength. Nat Neurosci 10:331–339.

Kang J, Jiang L, Goldman SA, Nedergaard M. 1998. Astrocyte-mediated potentiation of inhibitory synaptic transmission. Nat Neurosci 1:683–692.

Klausberger T, Magill PJ, Marton LF, Roberts JD, Cobden PM, Buzsaki G, Somogyi P. 2003. Brain-state- and cell-type-specific firing of hippocampal interneurons in vivo. Nature 421:844−848.

Kozlov AS, Angulo MC, Audinat E, Charpak S. 2006. Target cell-specific modulation of neuronal activity by astrocytes. Proc Natl Acad Sci USA 103:10058–10063.

Li X, Zima AV, Sheikh F, Blatter LA, Chen J. 2005. Endothelin-1-induced arrhythmogenic Ca^{2+} signaling is abolished in atrial myocytes of inositol-1,4,5-trisphosphate(IP_3)-receptor type 2-deficient mice. Circ Res 96:1274–1281.

Losi G, Mariotti L, Carmignoto G. 2014. GABAergic interneuron to astrocyte signalling: A neglected form of cell communication in the brain. Philos Trans R Soc Lond B Biol Sci 369:20130609.

Meier SD, Kafitz KW, Rose CR. 2008. Developmental profile and mechanisms of GABA-induced calcium signaling in hippocampal astrocytes. Glia 56:1127–1137.

Mori T, Tanaka K, Buffo A, Wurst W, Kuhn R, Gotz M. 2006. Inducible gene deletion in astroglia and radial glia–a valuable tool for functional and lineage analysis. Glia 54:21–34.

Navarrete M, Araque A. 2010. Endocannabinoids potentiate synaptic transmission through stimulation of astrocytes. Neuron 68:113–126.

Navarrete M, Perea G, de Sevilla DF, Gomez-Gonzalo M, Nunez A, Martin ED, Araque A. 2012. Astrocytes mediate in vivo cholinergic-induced synaptic plasticity. PLoS Biol 10:e1001259.

Nestor MW, Mok LP, Tulapurkar ME, Thompson SM. 2007. Plasticity of neuron-glial interactions mediated by astrocytic EphARs. J Neurosci 27: 12817–12828.

Nilsson M, Eriksson PS, Ronnback L, Hansson E. 1993. GABA induces Ca^{2+} transients in astrocytes. Neuroscience 54:605–614.

Nimmerjahn A, Kirchhoff F, Kerr JN, Helmchen F. 2004. Sulforhodamine 101 as a specific marker of astroglia in the neocortex in vivo. Nat Methods 1:31–37.

Parpura V, Grubisic V, Verkhratsky A. 2011. Ca^{2+} sources for the exocytotic release of glutamate from astrocytes. Biochim Biophys Acta 1813:984–991.

Perea G, Navarrete M, Araque A. 2009. Tripartite synapses: Astrocytes process and control synaptic information. Trends Neurosci 32:421–431.

Petersen CC, Crochet S. 2013. Synaptic computation and sensory processing in neocortical layer 2/3. Neuron 78:28–48.

Pierce KL, Premont RT, Lefkowitz RJ. 2002. Seven-transmembrane receptors. Nat Rev Mol Cell Biol 3:639–650.

Pirttimaki TM, Codadu NK, Awni A, Pratik P, Nagel DA, Hill EJ, Dineley KT, Parri HR. 2013. 7 Nicotinic receptor-mediated astrocytic gliotransmitter release: Aβ effects in a preclinical Alzheimer's mouse model. PLoS One 8: e81828.

Reyes-Haro D, Muller J, Boresch M, Pivneva T, Benedetti B, Scheller A, Nolte C, Kettenmann H. 2010. Neuron-astrocyte interactions in the medial nucleus of the trapezoid body. J Gen Physiol 135:583–594.

Serrano A, Haddjeri N, Lacaille JC, Robitaille R. 2006. GABAergic network activation of glial cells underlies hippocampal heterosynaptic depression. J Neurosci 26:5370–5382.

Sharp AH, Nucifora FC, Jr., Blondel O, Sheppard CA, Zhang C, Snyder SH, Russell JT, Ryugo DK, Ross CA. 1999. Differential cellular expression of isoforms of inositol 1,4,5-triphosphate receptors in neurons and glia in brain. J Comp Neur 406:207–220.

Shigetomi E, Bowser DN, Sofroniew MV, Khakh BS. 2008. Two forms of astrocyte calcium excitabilty have distinct effects on NMDA receptor-mediated slow inward currents in pyramidal neurons. J Neurosci 28:6659–6663.

Sohal VS, Zhang F, Yizhar O, Deisseroth K. 2009. Parvalbumin neurons and gamma rhythms enhance cortical circuit performance. Nature 459: 698–702.

Stark E, Eichler R, Roux L, Fujisawa S, Rotstein HG, Buzsaki G. 2013. Inhibition-induced theta resonance in cortical circuits. Neuron 80:1263–1276.

Varga C, Golshani P, Soltesz I. 2012. Frequency-invariant temporal ordering of interneuronal discharges during hippocampal oscillations in awake mice. Proc Natl Acad Sci USA 109:E2726–E2734.

Velez-Fort M, Audinat E, Angulo MC. 2011. Central role of GABA in neuron-glia interactions. Neuroscientist 18:237–250.

Verkhratsky A, Rodriguez JJ, Parpura V. 2012. Calcium signalling in astroglia. Mol Cell Endocrinol 353:45–56.

Verkhratsky A, Steinhauser C. 2000. Ion channels in glial cells. Brain Res Brain Res Rev 32:380–412.

Volterra A, Meldolesi J. 2005. Astrocytes, from brain glue to communication elements: The revolution continues. Nat Rev Neurosci 6:626–640.

Westenbroek RE, Bausch SB, Lin RC, Franck JE, Noebels JL, Catterall WA. 1998. Upregulation of L-type Ca^{2+} channels in reactive astrocytes after brain injury, hypomyelination, and ischemia. J Neurosci 18:2321–2334.

Zeng W, Mak DO, Li Q, Shin DM, Foskett JK, Muallem S. 2003. A new mode of Ca^{2+} signaling by G protein-coupled receptors: Gating of IP_3 receptor Ca^{2+} release channels by Gβγ. Curr Biol 13:872–876.